Journal of Power Sources 250 (2014) 236–241

Contents lists available at ScienceDirect

Journal of Power Sources

journal homepage: www.elsevier.com/locate/jpowsour

Interfacial interactions between an alkali-free borosilicate viscous sealing glass and aluminized ferritic stainless steel

Jen-Hsien Hsu [a], Cheol-Woon Kim [b], Richard K. Brow [a,*]

[a] Material Research Center, Missouri University of Science and Technology, Rolla, MO 65409, USA
[b] Mo-Sci Corporation, 4040 HyPoint North, Rolla, MO 65401, USA

ARTICLE INFO

Article history:
Received 25 September 2013
Received in revised form
4 November 2013
Accepted 11 November 2013
Available online 19 November 2013

Keywords:
Solid oxide fuel cell
Aluminized stainless steel
Interfacial interaction
Viscous sealing glass

ABSTRACT

An alkali-free, alkaline earth borosilicate glass (designated G73) has been developed as a viscous sealant for use with solid oxide fuel cells (SOFC). In this work, the interfacial interactions that occur between this viscous sealant and aluminized ferritic stainless steel (SS441) under SOFC operational conditions are described. YSZ/glass/aluminized SS441 sandwich seals were held at 800 °C in air for up to 1000 h, and the interfaces were analyzed using analytical scanning electron microscopy (ASEM). Interfacial reactions were also characterized by X-ray diffraction (XRD) analyses of heat-treated mixtures of glass and alumina powders. The results show that the glass reacted with aluminum from the steel to form $BaAl_2Si_2O_8$ crystals at the glass/metal interface and that the aluminum concentration in the aluminized steel was significantly depleted with time.

1. Introduction

Seals are required in the design of planar solid oxide fuel cells (SOFC) to prevent mixing of the fuel and oxidant, to provide mechanical bonding of components, and to provide electrical insulation between stack components. Sealants must be chemically and physically stable under the SOFC operating conditions, and it is still a challenge to develop sealing materials that meet the stringent design lifetimes for planar SOFC which may operate for ≥40,000 h with possibly hundreds of thermal cycles, in both the oxidizing and reducing atmospheres [1–3].

Glasses, including rigid and compliant (or viscous) designs, are the most common hermetic seals for SOFCs, because of tailored properties, like the coefficient of thermal expansion (CTE) and glass transformation temperature (T_g), low cost and convenient processibility [4–6]. Alkaline earth aluminosilicate glass–ceramics are typical rigid seals for SOFC applications, because of their CTE match to other SOFC materials [3,7–9]. Compliant sealing glasses [10–12] are designed to be viscous at the SOFC operating and have the potential to "self-heal" cracks generated during thermal cycling.

Interfacial interactions between glass seals and the Cr_2O_3-forming stainless steel interconnects may degrade seal quality. Alkali components in sealants may react with the interconnects to form volatile $Na_2CrO_4(g)$ and $K_2CrO_4(g)$, which causes Cr to deposit on the cathode, blocking active sites [2,13,14]. Under oxidizing conditions, alkaline earth silicate glasses can react with interconnects to form deleterious high expansion chromates, i.e. $BaCrO_4$ (CTE $>16 \times 10^{-6}$ °C^{-1}) [15–17] and $SrCrO_4$ (CTE $\sim 22 \times 10^{-6}$ °C^{-1}) [18], and generate interfacial porosity [15]. Protective coatings, including, alumina [14,19,20], $(Mn, Co)_3O_4$ [19] and YSZ [21,22] have been investigated to improve the stability and reduce Cr volatility from the interconnects under SOFC operational conditions.

In the present study, the long-term interactions at 800 °C in air between a newly developed, alkali-free viscous sealing glass and both aluminized SS441 and Y-stabilized zirconia were studied. Of particular interest is the incorporation of aluminum from the steel into the glass and its effect on the long-term crystallization of the glass.

2. Experimental procedure

2.1. Glass composition and properties

The glass, designated G73, used in this study is an alkali-free, alkaline earth aluminum borosilicate (Ba–Ca–Sr–Al–Si–B) designed by Missouri S&T and MO-SCI Corporation. A homogeneous mixture of the appropriate raw materials was melted in a

* Corresponding author. 101 Straumanis-James Hall, 401 W. 16th St., Rolla, MO 65409-0330, USA. Tel.: +1 573 3416812; fax: +1 573 3416934.
E-mail address: brow@mst.edu (R.K. Brow).

0378-7753/$ – see front matter © 2013 Elsevier B.V. All rights reserved.
http://dx.doi.org/10.1016/j.jpowsour.2013.11.018

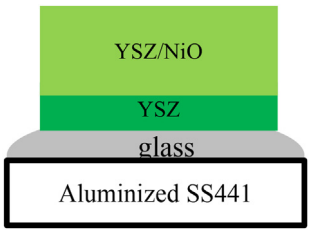

Fig. 1. Schematic diagram of the sandwich seals. The ratios of layer thickness are not representative of the actual samples.

silica crucible (99.6% SiO_2, 0.2% Al_2O_3) at 1100 °C for 7 h in air. The melt was stirred 3–4 times over a period of 30 min, then quenched onto a clean steel plate. The glass has a glass transition temperature (T_g) of ~624 °C, Littleton softening temperature (viscosity equals $10^{6.6}$ Pa-s) of ~706 °C, glass liquidus temperature (T_L) of ~800 °C, and thermal expansion coefficient (CTE) of ~8.5×10^{-6} °C^{-1}. Information about the preparation and properties of this glass is given in Ref. [12].

2.2. SOFC sandwich seals

G73 was used to make sandwich seals between aluminized SS441 and a YSZ/NiO-YSZ bilayer, both provided by Pacific Northwest National Laboratory (PNNL) (Fig. 1). SS441, a ferritic stainless steel, is a candidate for the interconnect material because it has a CTE match to YSZ anode support, it forms an electrically conducting oxide scale, and it has a relatively low cost [11]. The nominal composition of SS441 is Fe (bal.), 17.5–19.5 wt.% Cr, with trace of Nb, Mn and Si [23]. The parts used in this study were aluminized using a reactive air aluminizing coating process developed by PNNL [19]. The SS441 substrates were sprayed with the solution consisting of a binder and a mixture of aluminum powders, followed by drying and oxidizing at 1000 °C for 1 h in air. A glass powder paste was made by mixing G73 powder (20–50 μm) with ethanol to get the desired consistency. The paste was applied to an aluminized SS441 substrate (25 mm × 15 mm × 1 mm), and the piece was slowly heated (1 °C min^{-1}) to 200 °C for 2 h then slowly cooled (~2 °C min^{-1}) to room temperature, before the YSZ bilayer (15 mm × 10 mm × 0.5 mm) was pressed into the dried paste. The assembly was then heated to 800 °C (20 °C min^{-1}) to form the YSZ bi-layer/glass/aluminized SS441 sandwich seal. The resulting final thickness of the glass layer was 150–250 microns.

To study the interfacial reactions, the sandwich samples were held in air at 800 °C (metal-side down) for designated times. After cooling (~2 °C min^{-1}), the sandwich samples were fixed in epoxy and cross-sectioned to examine the interfaces. The samples were prepared following normal metallography procedures. Microstructure and compositional characterization of samples were done by scanning electron microscopy (Helios NanoLab 600 FIB/FESEM) with energy dispersive spectroscopy (EDS). Quantitative image analyses were done on some micrographs using the Image J 1.45s software package.

2.3. Glass/alumina reactions

Glass (G73) powders (<35 μm) were mixed with alumina (99.5%) powders (<35 μm) in a 1:1 weight ratio in a 250 mL plastic jar with ZrO_2 milling cylinders and ethanol. The powder mixtures were ball milled for 2 h, followed by drying on a hot-plate. The mixed powders were die-pressed at 20 MPa into pellets (dia.: 12.7 mm, thickness: ~4 mm), the pellets were held at 800 °C for 14 days in air. The heat-treated pellets were ground to powders (<150 μm) and analyzed using X-ray diffraction (Philips X-Pert Diffractometer).

In a second experiment, a 50 mL alumina (99.6%) crucible with 50 g of glass (G73) was held at 800 °C in air for 1000 h. This sample was slowly cooled (~2 °C min^{-1}) and sectioned to examine the glass/alumina interface using scanning electron microscopy.

Finally, three glasses in addition to G73 were prepared with 50%, 100% and 200% excess Al_2O_3 compared with the baseline G73 composition, using the preparation procedures described in Ref. [12]. About 15 g of each glass were held at 800 °C in a platinum crucible in air for seven days, then quenched in water. Glass pieces from the center of each sample, and from the glass/air and glass/Pt interfaces were selected, then fixed in epoxy and sectioned for SEM analyses.

3. Results

3.1. Aluminized stainless steel 441 (SS441)

Fig. 2 shows a cross-section of the as-received aluminized SS441 samples. There is an Al-rich oxide surface layer about 1–2 μm thick

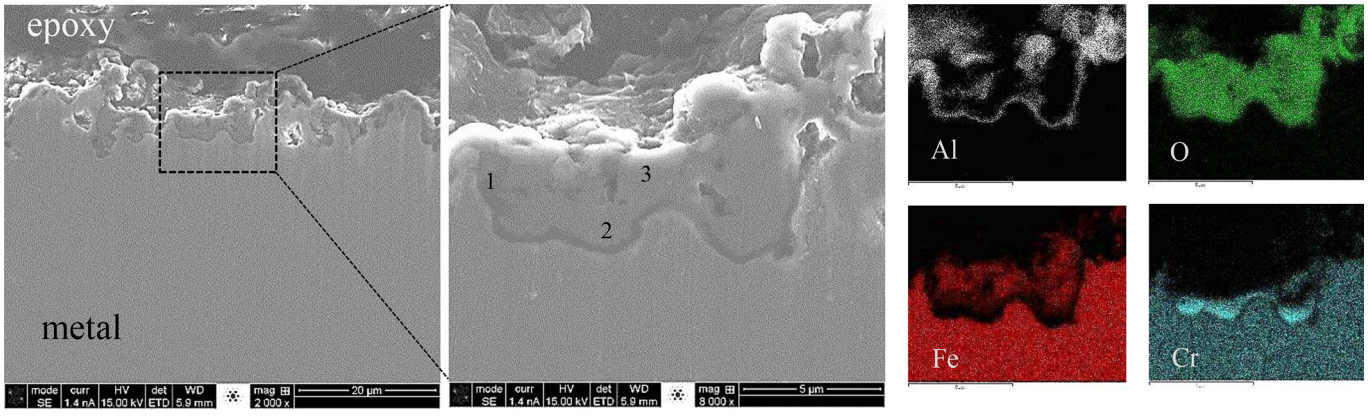

Fig. 2. (a and b) Micrographs and (c) elemental mapping (EDS) of aluminized SS441 (as-received from PNNL). The image in the center (b) is a high magnification view of the area indicated in the image on the left (a). Elemental concentrations of the three points indicated in image (b) are given in Table 1.

Table 1
Chemical composition (by EDS; in at.%) of the spots indicated in Fig. 2.

	O	Al	Fe	Cr
1	56	21	9	13
2	61	5	16	17
3	62	5	31	1

immediately adjacent to the underlying metal and an outer layer (2–5 μm thick) of mixture of Al-rich and (Fe, Cr)-rich oxides. The composition of the (Fe, Cr)-rich oxides, determined by EDS, is not uniform (Fig. 2 and Table 1). The presence of Fe-rich and Cr-rich oxide layers above the Al-rich layer was also reported by PNNL [11]. Below the alumina layer is a subsurface aluminum reservoir layer, about 100 μm deep with ~13 at.% Al at the oxide/metal interface (Fig. 3(a)). The Al-concentration profiles in the aluminized SS441 were measured on both the air-side and glass-side for sandwich samples held at 800 °C for different times, from 3 days to ~42 days (1000 h); these are shown as the data points in Fig. 3(a) and (b), respectively. It is significant that the Al-concentration decreased with heat treatment time at both surfaces, and the depletion of Al from the glass-side is faster than from the air-side. In addition, a comparison of the cross-sections of aluminized SS441 substrates 'as received' (Fig. 2(a)) and after 1000 h at 800 °C in air (Fig. 4) shows that there are no significant differences in the thickness of the oxide surface layers.

3.2. SS441/G73/YSZ interfaces

Fig. 5 shows representative images of the cross-section of an aluminized SS441/G73/YSZ sandwich seal after 1000 h at 800 °C in air. There is complete wetting and good bonding of the glass at both the glass/YSZ and glass/metal interfaces. The horizontal crack through the glass was created during the preparation of this cross-sectioned sample. Similar sandwich seals remain hermetic after

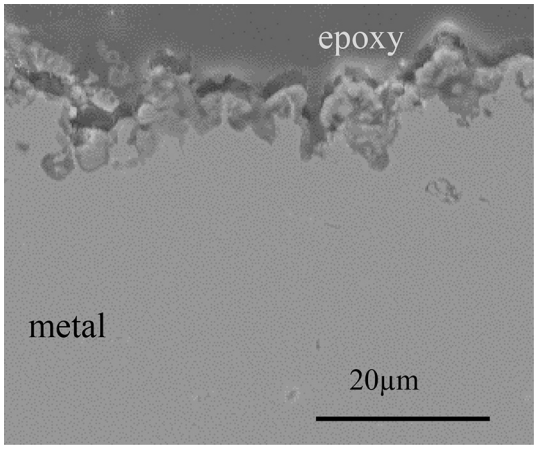

Fig. 4. Cross-section micrograph of the air-side of SS441 heat-treated for 1000 h at 800 °C.

rapid quenches (~25 °C s^{-1}) from 800 °C or after 100 thermal cycles between 750 °C and room temperature [12]. After 1000 h at 800 °C, the 1–2 μm thick Al-rich oxide surface layer still exists immediately adjacent to the underlying steel (Fig. 6(b)). Some barium silicate crystals formed in glass layer (Fig. 5(a)) and EDS indicates that the composition of those crystals are 10% Ba, 10% Si, 2% Ca, 4% Sr and 72% O (atom%), although boron cannot be detected by the EDS system used.

In the glassy layer adjacent to the metal, needle-like crystals are apparent (Fig. 6(a)) and these crystals are more Al-rich (Table 2) than those barium silicate crystals in the center of the glass. After 1000 h, the Al-rich crystals have become larger and more platy-shaped (Fig. 6(b)).

There is little evidence for interactions between G73 and YSZ after 1000 h at 800 °C (Fig. 5(b)). No zirconium or yttrium was

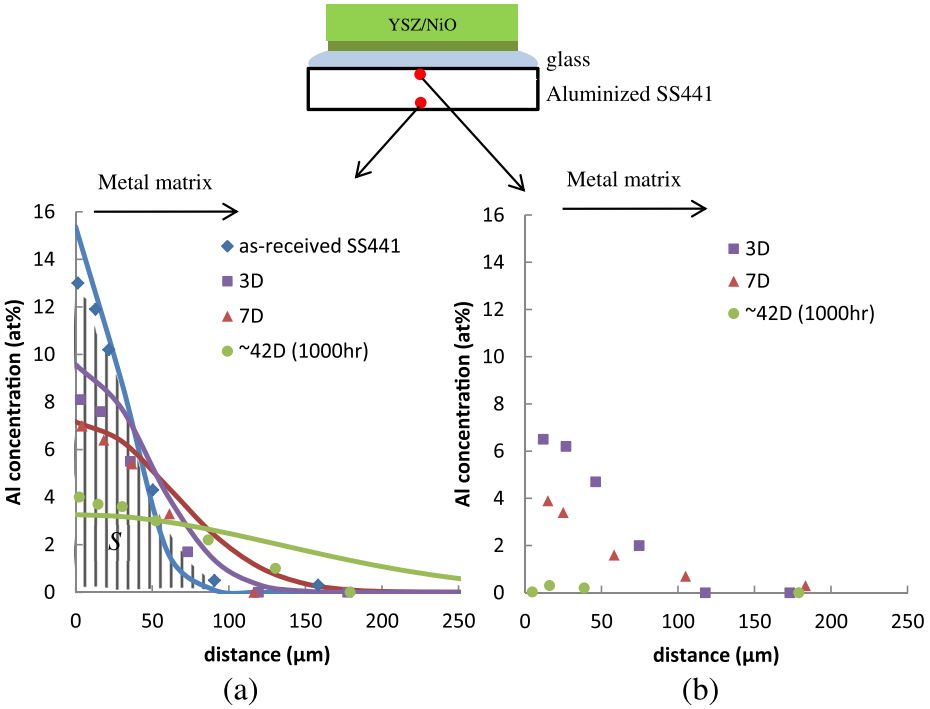

Fig. 3. Measured (symbols) and calculated (solid lines, from Equation (2)) aluminum diffusion profiles from metal surfaces on the (a) air-side, and (b) glass-side for sandwich seals heat-treated at 800 °C in air for different times.

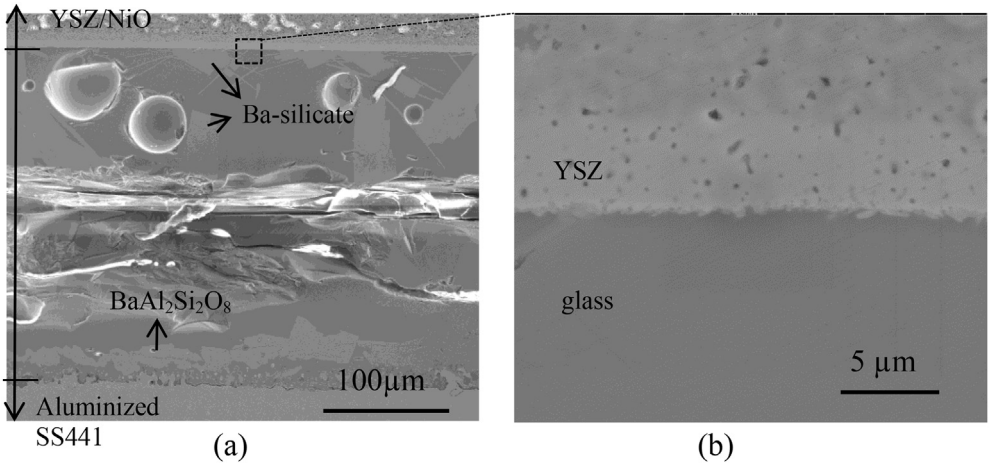

Fig. 5. Micrographs of an SOFC sandwich seal after 1000 h at 800 °C in air. The image on the right (b) is a high magnification view of the area indicated in the image on the left (a).

detected in glass and no Zr- or Y-containing crystals were observed at the glass/YSZ interface.

3.3. Glass/alumina reactions

Fig. 7 shows the XRD pattern from the glass–alumina reaction couple after 14 days at 800 °C in air. In addition to the peaks due to unreacted alumina powder, the monoclinic and hexagonal phases of $BaAl_2Si_2O_8$ were detected.

Fig. 8 shows the micrograph and EDS-mapping of the interface between the glass and the alumina crucible after 1000 h at 800 °C in air. These crystals, which are rich in Al, Si and Ba, formed over the entire glass/alumina interface, but not in the bulk of the glass. Also, the stoichiometry of the crystals, determined by EDS, is close to $BaAl_2Si_2O_8$ (Table 2).

4. Discussion

Viscous sealing glasses are of interest for SOFC designs because cracks that might form in the seal due to thermal stresses during temperature cycling may reseal through viscous flow upon re-heating [17,24]. For example, test seals between aluminized SS441 and YSZ bilayers made with G73, purposefully cracked by quenching samples from 800 °C to room temperature were resealed when reheated to temperatures as low as 725 °C [12]. However, interfacial reactions between a viscous sealing glass and the SOFC components are likely to be more severe than those involving a rigid glass–ceramic because of faster diffusion kinetics associated with a lower viscosity material, and so the effects of those reactions on seal performance must be determined.

In the present work, it is hypothesized that $BaAl_2Si_2O_8$ crystals form near the glass/metal interface because of the reaction between components in the glass and the aluminized SS441. Specifically, alumina is dissolved from the metal into the glass and the $BaAl_2Si_2O_8$ crystals then precipitate from the Al-rich melt.

The needle-shaped $BaAl_2Si_2O_8$ crystals are present only in the G73 glass when it reacts with the aluminized steel or when it is in contact with the dense alumina crucible or with the alumina powder. These crystals do not form when the G73 glass is heated in platinum.

Because there is no significant oxide growth on the air-side of the aluminized SS441, even after 1000 h at 800 °C (Fig. 4), the changes in the Al-concentration gradients on the air-side (Fig. 3(a)) are assumed to result from Al diffusion from the subsurface into the metal matrix. This process can be described using a simple model based on "diffusion from a limited source" [25]. The assumptions in this model include a non-moving interface (metal/oxide), no Al diffusion from the oxide into the metal or from the metal into the oxide, and the steel matrix acts as a semi-infinite sink for Al diffusion. The concentration (C) of the diffusing species (Al) as a

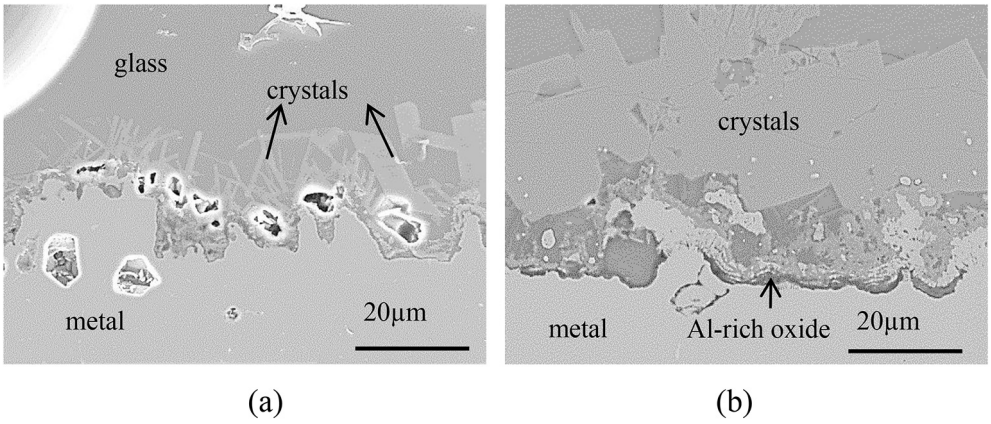

Fig. 6. Micrographs of the glass/metal interface of an SOFC sandwich seal after (a) 7 days and (b) ~42 days (1000 h) at 800 °C in air. The average composition of the crystals indicated is given in Table 2.

Table 2
Chemical composition (by EDS) of barium aluminum silicate crystals formed at 800 °C for the designated time.

Composition (at.%)				Remark
O	Al	Si	Ba	
61.5	15.4	15.4	7.7	Stoichiometric $BaAl_2Si_2O_8$
68	13	12	6	Sandwich seal, 7 days
63	15	14	8	Sandwich seal, ~42 days
62	16	15	7	Glass#73 in alumina crucible, 14 days
63	15	15	7	Glass#73 + 50% excess Al_2O_3 in Pt crucible, 7 days
63	14	15	8	Glass#73 + 100% excess Al_2O_3 in Pt crucible, 7 days
63	14	15	8	Glass#73 + 200% excess Al_2O_3 in Pt crucible, 7 days

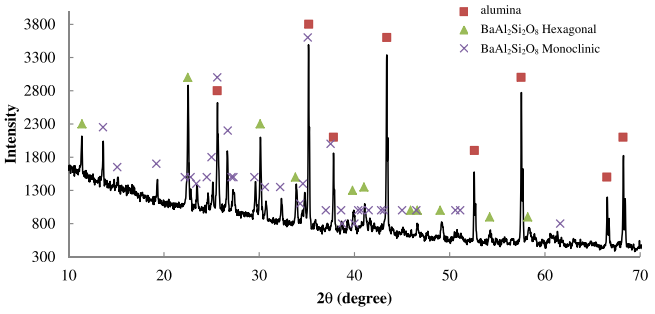

Fig. 7. XRD pattern of mixture of glass (G73) and alumina powders heat-treated for 14 days at 800 °C in air.

function of time (t) and distance from the interface (x) can be thus described by

$$\int_0^\infty C(x,t)\mathrm{d}x = S \quad (1)$$

where S is a constant value, and

$$C(x,t) = \frac{S}{\sqrt{\pi Dt}}\exp\left(\frac{-x^2}{4Dt}\right) \quad (2)$$

where D is the diffusion coefficient. The Al profile of the as-received SS441 in Fig. 3(a) was calculated starting with a pure Al (thin film) diffusion source with an amount S defined by the total Al in the diffusion profile (Fig. 3(a)), the reported diffusion coefficient for Al in a Fe–20Cr–5Al alloy at 1000 °C (1.1×10^{-9} cm^2 s^{-1}) [27], and a time of 1 h; this temperature and time are the aluminization processing conditions reported by PNNL [26]. (PNNL heats and cools the aluminized samples at 3 °C min^{-1} around the 1 h soak; Al diffusion during the heating and cooling steps was ignored.) For the diffusion profiles of the heat-treated samples, the same value for S was used as indicated above, with a diffusion coefficient of 2.4×10^{-11} cm^2 s^{-1} at 800 °C [27]. The 'as received' Al-profile, created by the original aluminization process, is equivalent to 50 h of diffusion at 800 °C from a pure aluminum source. This 'baseline time' was then added to the experimental time when calculating the Al profiles of the heat-treated samples shown in Fig. 3(a); e.g., the 7 day (168 h) profile is calculated using 218 h in Equation (2).

Fig. 3(a) shows that the calculated diffusion profiles (lines from Equation (2)) are in reasonable agreement with the experimental results (symbols). The similar Al diffusion depth at both the air-side and the glass-side interfaces and the more rapid depletion of Al at the glass-side interface implies that Al is not diffusing deeper into the metal as it is at the air-side, but instead is preferentially diffusing from the metal into the glass. Also, there is no evidence for a retreat of the metal surface at either interface. If the Al-rich region dissolved into the glass, then large concentrations of Fe and Cr should also be present, and this was not observed.

Image analyses of micrographs like those in Fig. 6 provided an estimate of the volume fraction of crystals that form in the glassy layer of the sandwich seals. With the assumption that the stoichiometry of these crystals is $BaAl_2Si_2O_8$, an estimate total concentration of Al present in these crystals can be made. This analysis revealed that 60–80% of the Al that migrated from the Al reservoir in the SS441 can be accounted for in the $BaAl_2Si_2O_8$ crystals. Although the details of the transfer and reaction mechanism are not clear, this result strongly implies that the aluminum reservoir of the SS441 is the major aluminum source for the formation of the $BaAl_2Si_2O_8$ crystals.

The addition of alumina to the G73 base glass leads to the precipitation of $BaAl_2Si_2O_8$ crystals at 800 °C. For example, the addition

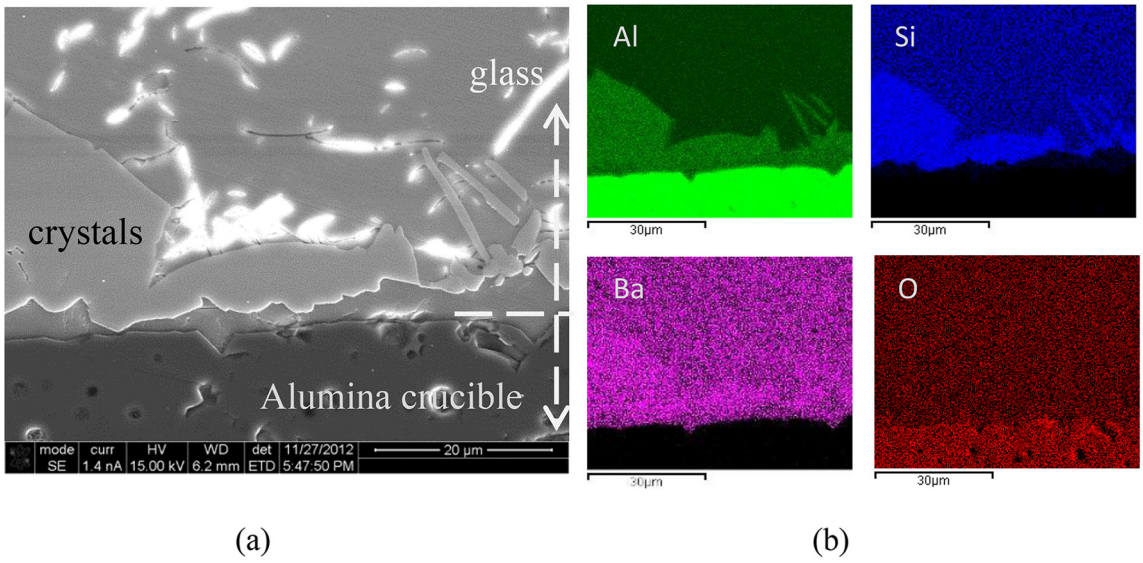

Fig. 8. (a) Micrograph and (b) elemental mapping (EDS) of the interface between G73 glass and an alumina crucible heat-treated for 1000 h at 800 °C in air. The average composition of the crystals indicated is given in Table 2.

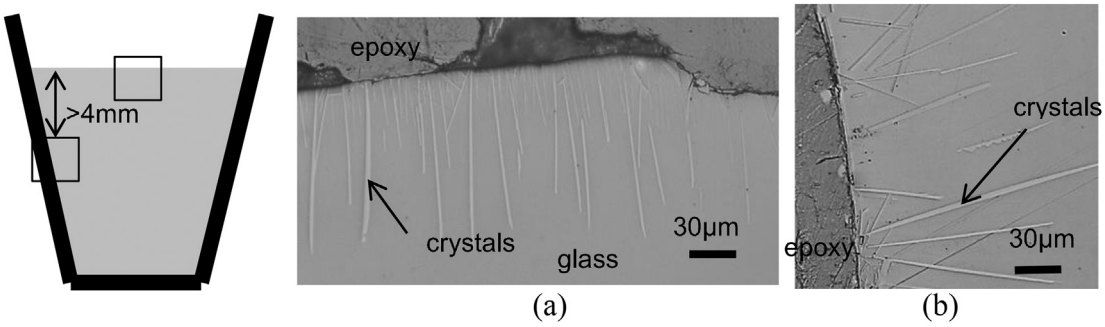

Fig. 9. Micrographs of G73 with 50% excess alumina after 7 days at 800 °C in platinum crucible in air. Image (a) shows a glass piece near the glass/air interface. Image (b) shows a glass piece near the glass/Pt interface. The average composition of the crystals indicated is given in Table 2.

of 50% excess alumina to G73 results in the formation of needle-shaped crystals associated with $BaAl_2Si_2O_8$ at the glass/air and glass/platinum interfaces after seven days at 800 °C in air (Fig. 9). EDS confirms the $BaAl_2Si_2O_8$ stoichiometry for these crystals, as well as the crystals in glasses with 100% and 200% excess Al_2O_3 (Table 2). These crystals could not be detected in the baseline G73 glass held in platinum under the same conditions.

There have been other reports of similar interactions between aluminized steel and silicate sealing glasses. Meinhardt et al. [1] detected a 2–3 μm thin $BaAl_2Si_2O_8$ scale at the interface of barium aluminosilicate glass and alumina-forming steel after 1 h at 850 °C in air. Chou et al. [11] reported that the alumina coating of aluminized stainless steel (SS441) was attacked by an alkali aluminosilicate glass after 500 h at 800 °C, producing a greater Al concentration in glass, promoting the precipitation of $KAlSi_3O_8$ crystals near the glass/steel interface.

The formation of $BaAl_2Si_2O_8$ under SOFC operational conditions might be detrimental to the long-term sealing performance of viscous sealing glasses because this phase has a lower CTE than the base glass; the CTEs of monoclinic and hexagonal forms of $BaAl_2Si_2O_8$ are 3×10^{-6} °C^{-1} and 8×10^{-6} °C^{-1}, respectively [20].

5. Conclusions

The interfacial interactions that occur between an alkaline earth alumino-borosilicate viscous sealing glass (G73) and aluminized stainless steel (SS441) can be summarized by the following:

- The surface Al concentration of the aluminized SS441 decreased with heat treatment time and this depletion could be modeled by the diffusion of Al into the steel matrix and the migration of the Al into the glass.
- The increase in local concentration of aluminum in the sealing glass caused crystals to form at the glass/aluminized steel interface and these crystals are most likely $BaAl_2Si_2O_8$.
- The $BaAl_2Si_2O_8$ crystals form at 800 °C when this glass reacts with alumina powder, at the interface with an alumina crucible, and when excess alumina is added to the base glass composition.

The consequences of these types of interfacial reactions on the long-term performance of viscous glass seals must be understood if aluminized steel is to be used for SOFC applications.

Acknowledgment

The authors would like to thank Yeong-Shyung. Chou and Jeffry W. Stevenson at PNNL for providing aluminized SS441 and YSZ/NiO-YSZ bilayer, and Eric Bohannan, Charmayne Smith and Kathryn Goetschius at Missouri S&T for XRD analyses. This work was supported by US Department of Energy under Contract # DE-SC0002491.

References

[1] K.D. Meinhardt, D.-S. Kim, Y.-S. Chou, K.S. Weil, J. Power Sources 182 (2008) 188–196.
[2] N. Lahl, L. Singheiser, K. Hilpert, Electrochem. Soc. Proc. 99-19 (1999) 1057–1066.
[3] J.W. Fergus, J. Power Sources 147 (2005) 46–57.
[4] K.L. Ley, M. Krumpelt, R. Kumar, J.H. Meiser, I. Bloom, J. Mater. Res. 11 (1996) 1489–1493.
[5] S.-B. Sohn, S.-Y. Choi, G.-H. Kim, H.-S. Song, G.-D. Kim, J. Non-cryst. Sol. 297 (2002) 103–112.
[6] P.A. Lessing, J. Mater. Sci. 42 (2007) 3465–3476.
[7] K.D. Meinhardt, J.D. Vienna, T.R. Armstrong, L.R. Pederson, U.S. Patent No. 6430966, 2002.
[8] N. Lahl, K. Singh, L. Singheiser, K. Hilpert, J. Mater. Sci. 35 (2000) 3089–3096.
[9] S.T. Reis, R.K. Brow, J. Mater. Eng. Perform. 15 (2006) 410–413.
[10] R.N. Singh, J. Mater. Res. 27 (2012) 2055–2061.
[11] Y.-S. Chou, J.-P. Choi, J.W. Stevenson, Int. J. Hydrogen Energy 37 (2012) 18372–18380.
[12] C.W. Kim, J.H. Hsu, C. Townsend, J. Szabo, R. Crouch, R. Baird, R.K. Brow, Ceram. Eng. Sci. Proc. 34 (4) (2013).
[13] K. Hilpert, D. Das, M. Miller, D.H. Peck, R. Wei, J. Electrochem. Soc. 143 (1996) 3642–3647.
[14] K. Ogasawara, H. Kameda, Y. Matsuzaki, T. Sakurai, T. Uehara, A. Toji, N. Sakai, K. Yamaji, T. Horita, H. Yokokawa, J. Electrochem. Soc. 154 (2007) B657–B663.
[15] Z. Yang, J.W. Stevenson, K.D. Meinhardt, Solid State Ionics 160 (2003) 213–225.
[16] V.A.C. Haanappel, V. Shemet, I.C. Vinke, S.M. Gross, T.H. Koppitz, N.H. Menzler, M. Zahid, W.J. Quadakkers, J. Mater. Sci. 40 (2005) 1583–1592.
[17] T. Zhang, R.K. Brow, W.G. Fahrenholtz, S.T. Reis, J. Power Sources 205 (2012) 301–306.
[18] Y.-S. Chou, J.W. Stevenson, P. Singh, J. Power Sources 184 (2008) 238–244.
[19] J.-P. Choi, K. Scott Weil, Y.-S. Chou, J.W. Stevenson, Z.-G. Yang, Int. J. Hydrogen Energy 36 (2011) 4549–4556.
[20] Y.-S. Chou, J.W. Stevenson, P. Singh, J. Power Sources 185 (2008) 1001–1008.
[21] P. Batfalsky, V.A.C. Haanappel, J. Malzbender, N.H. Menzler, V. Shemet, I.C. Vinke, R.W. Steinbrech, J. Power Sources 155 (2006) 128–137.
[22] Y.-S. Chou, E.C. Thomsen, J.-P. Choi, J.W. Stevenson, J. Power Sources 197 (2012) 154–160.
[23] S.D. Washko, G. Aggen, ASM Handbook, vol. 1, ASM International, 1990, pp. 841–907.
[24] R.N. Singh, Int. J. Appl. Ceram. Technol. 4 (2007) 134–144.
[25] R.W. Balluffi, S.M. Allen, W.C. Carter, Kinetics of Materials, first ed., John Wiley & Sons Int., New Jersey, 2005.
[26] J.P. Choi, Y.S. Chou, J.W. Stevenson, Reactive Air Aluminization, 2011. PNNL-20859.
[27] A. Heesemann, E. Schmidtke, F. Faupel, Scr. Mater. 40 (1999) 517–522.